Minimum switching control for spacecraft precision pointing with on/off actuators

Mirko Leomanni[1], Andrea Garulli[1], Antonio Giannitrapani[1], Fabrizio Scortecci[2]

Abstract— **Maintaining the spacecraft attitude precisely aligned to a given orientation, while rejecting a persistent disturbance, using on/off actuators, is crucial for missions involving electric propulsion spacecraft. The objective is to enforce an oscillating attitude motion about the setpoint, so as to simultaneously minimize both the propellant consumption and the switching frequency of the control system. This paper evaluates the feasibility of a recently proposed feedback control law for this problem. This techniques is able to track both the period and the phase of periodic oscillations along the rotational axes, which is instrumental to minimize the switching frequency in the presence of input coupling. Two simulation case studies of a low Earth orbit missions are considered, showing that the proposed approach can effectively deal with both constant and time-varying disturbance torques.**

I. Introduction

All-electric spacecraft missions are receiving increasing attention from the aerospace community, see e.g. [1], [2]. Among the many advantages brought by this technological solution, there is the possibility of exploiting the same propellant bus for both orbit transfer maneuvers and precise attitude regulation, thus reducing costs and providing an effective alternative to momentum exchange devices [3], [4], [5]. Recent developments of high temperature resistojets and hollow cathode technologies [6], [7], providing a much higher specific impulse with respect to existing microthrusters, further motivates the study of attitude regulation schemes based on electric propulsion. On the other hand, these thrusters present some severe restrictions, the most important one concerning the fact that they must be operated in on/off mode, which clearly limits the control authority. Moreover, the switching frequency can have a significant impact on the performance and the lifetime of this type of actuators.

The presence of several disturbance torques affecting the attitude dynamics, due, e.g., to orbit control thruster misalignment or environmental sources, calls for a control law adopting some kind of pulse modulation in order to compensate for the disturbance on average. Therefore, an oscillating motion about the setpoint must be accepted. In designing this motion, the minimization of both the fuel consumption and the on/off switching frequency of the control system must be pursued. Optimal control of switching systems has been intensively investigated (see, e.g., [8], [9]), but very few contributions have addressed explicitly the minimization of the switching frequency [10], [11], [5]. In the considered application, this problem becomes challenging when the control design cannot be decoupled along the principal axes of inertia, due to the chosen thruster configuration. Moreover, the methods cited above involve a high computational burden, which may not fit the processing power available onboard a spacecraft. In [12], a periodic suboptimal solution to the minimum switching problem has been derived, for the case of coupled double integrators. It has been shown that a relative phase difference must be enforced among the trajectories of the integrators, in order to minimize the switching frequency, while satisfying given control accuracy requirements. In [13] a feedback control law has been proposed that can be used to steer the dynamics of the double integrator model to limit cycle oscillations with prescribed period and phase.

In this paper, the feasibility of the control law proposed in [13] is demonstrated on a spacecraft attitude regulation problem, within a low Earth orbit mission (LEO), in the presence of constant or time-varying disturbances. Although the considered control law, consisting of a relay feedback element with time-varying hysteresis for each rotational axis, has been originally designed for a constant disturbance, simulation results show that it is able to compensate also slowly time-varying disturbance torques. It turns out that the attitude dynamics, simulated through the full nonlinear model, are indeed steered to the desired periodic solution, and the actuator switching frequency is significantly smaller than that achieved by a control law which does not track the relative phases.

The paper is organized as follows. In Section II, the attitude dynamic model is introduced, along with the main features of the control problem. In Section III, the minimum fuel/switching control law under consideration is briefly recalled. The performance of the proposed approach is evaluated through numerical simulations of a LEO mission in Section IV, while some concluding remarks are given in Section V.

II. Problem setting

In this section, the model describing the attitude error dynamics is introduced, and the attitude regulation problem is formulated. The orientation of reference frame B with respect to a reference frame A is represented by the quaternion $q_{AB} = [\,\rho_{AB},\, \vec{q}_{AB}^{\,T}\,]^T$, where ρ_{AB} and $\vec{q}_{AB}$ are the scalar part and the vector part of the quaternion. The quaternion

[1]M. Leomanni, A. Garulli and A. Giannitrapani are with the Dipartimento di Ingegneria dell'Informazione e Scienze Matematiche, Università di Siena, Siena, Italy. Email: {leomanni,garulli,giannitrapani}@dii.unisi.it.

[2]F. Scortecci is with Aerospazio Tecnologie s.r.l., Rapolano Terme, Siena, Italy. Email: fscortecci@aerospazio.com.

multiplication $q_{AC} = q_{BC} \circ q_{AB}$ is defined by

$$q_{AC} = \begin{bmatrix} \rho_{BC}\rho_{AB} - \vec{q}_{BC}^T\vec{q}_{AB} \\ \rho_{BC}\vec{q}_{AB} + \rho_{AB}\vec{q}_{BC} - \vec{q}_{BC} \times \vec{q}_{AB} \end{bmatrix},$$

where $\times$ denote the cross product operation. The skew-symmetric matrix constructed from a vector ω is denoted by $\omega^\times$, u_j indicates the j-th entry of vector u, and $\|\cdot\|_\infty$ denotes the maximum norm of a vector.

A. Attitude error dynamics

The attitude of a spacecraft is commonly described as the orientation of a reference frame centered at center of mass and aligned with the principal axes of inertia of the body, which is termed as the body frame, with respect to an inertial frame. Let the orientation of the body frame with respect to the inertial frame be denoted by the four-dimensional quaternion q_{IB}, and the angular rate of the body frame with respect to inertial frame, expressed in the body frame, be denoted by the three-dimensional vector ω_B. The kinematics of the attitude quaternion are given by

$$\dot{q}_{IB} = \frac{1}{2} \begin{bmatrix} 0 \\ \omega_B \end{bmatrix} \circ q_{IB}. \tag{1}$$

Under the rigid body assumption, the angular rate dynamics are given by

$$\dot{\omega}_B = I_M^{-1} \left(\tau - \omega_B \times I_M\, \omega_B\right). \tag{2}$$

where I_M is the inertia matrix of the body and

$$\tau = \tau_d + \tau_u \tag{3}$$

denotes the torque acting on the system, including a disturbance torque τ_d and a control torque τ_u.

The desired attitude is specified by the orientation q_{IR} of a target reference frame with respect to the inertial frame and by the angular velocity ω_R of the target frame with respect to the inertial frame, expressed in the target frame. Let q_{RI} denote the inverse rotation of q_{IR}. Using quaternion algebra, the attitude error q_{RB}, which indicates the orientation of the body frame relative to the target frame, can be expressed as $q_{RB} = q_{IB} \circ q_{RI}$. If the attitude error is small, it can be approximated by the three-dimensional rotation vector $\delta\theta$, which is obtained from the vector part $\vec{q}_{RB}$ of the attitude error quaternion as

$$\delta\theta = 2\vec{q}_{RB}. \tag{4}$$

Now, let us define

$$\delta\omega = \omega_B - \omega_R. \tag{5}$$

For small $\delta\theta$ and $\delta\omega$, the evolution of (4) can be approximated by a linearized model. The linearized kinematic model is obtained by differentiating (4) and linearizing the resulting expression [14], thus obtaining the Bortz equation

$$\delta\dot{\theta} = \delta\omega - \omega_R^\times \delta\theta, \tag{6}$$

where the term $\omega_R^\times\delta\theta$ accounts for the fact that ω_B and ω_R in (5) are expressed in two different, possibly rotating, frames. By differentiating (5) with respect to time and exploiting (2), one gets

$$\delta\dot{\omega} = I_M^{-1}\tau - I_M^{-1}(\omega_R + \delta\omega)^\times I_M(\omega_R + \delta\omega) - \dot{\omega}_R. \tag{7}$$

In most practical applications, the target frame is either spinning at a constant angular velocity or inertially fixed. In the first case, the linearized dynamic model is found by enforcing $\dot{\omega}_R = 0$ in (7) and linearizing the resulting expression about $\delta\omega = 0$, yielding

$$\delta\dot{\omega} = A\delta\omega + I_M^{-1}\tau, \tag{8}$$

where

$$A = \begin{bmatrix} 0 & \frac{\iota_2-\iota_3}{\iota_1}\omega_3 & \frac{\iota_2-\iota_3}{\iota_1}\omega_2 \\ \frac{\iota_3-\iota_1}{\iota_2}\omega_3 & 0 & \frac{\iota_3-\iota_1}{\iota_2}\omega_1 \\ \frac{\iota_1-\iota_2}{\iota_3}\omega_2 & \frac{\iota_1-\iota_2}{\iota_3}\omega_1 & 0 \end{bmatrix}, \tag{9}$$

ι_j denotes the principal moments of inertia, $\omega_R = [\omega_1, \omega_2, \omega_3]^T$ and $I_M = \mathrm{diag}(\iota_1, \iota_2, \iota_3)$. For the case in which the reference attitude is inertially fixed, one has that $\omega_R = 0$ in (6) and (8)-(9). Hence, the error dynamics take on the form of the double integrator system

$$\delta\ddot{\theta} = I_M^{-1}\tau. \tag{10}$$

Notice that, under the assumption of small attitude errors, (10) provides a valid approximation of the dynamics (6),(8), as long as ω_R is small. In this paper, model (10) will be used to design the control law to be applied to system (1)-(3) for disturbance rejection and attitude regulation.

B. Minimum switching control problem

The considered control problem consists of tracking the desired attitude q_{IR}, using a set of on/off actuators mounted at a fixed orientation with respect to the body frame. For this design, the control torque τ_u in (3) can be expressed as

$$\tau_u = B\,\mu, \tag{11}$$

where $\mu \in \{-1, 0, 1\}^3$ indicates the on/off actuator command and the matrix B expresses the linear mapping from this command to the control torque. Due to the presence of integer inputs and of the disturbance term τ_d in (3), affecting the attitude dynamics, the tracking error (4) cannot be steered exactly to the origin (an infinite switching frequency would be required). Instead, an oscillating motion of prescribed amplitude about the setpoint must be accepted. Hence, the objective of the control system is to guarantee that

$$\|W\,\delta\theta(t)\|_\infty \leq 1, \quad \forall t \geq \bar{t}, \tag{12}$$

for some $\bar{t} \geq 0$, where the weighting matrix W, specifying the maximum allowed deviation from the setpoint, is usually diagonal.

The minimization of both the fuel consumption and the on/off switching frequency of the actuators is a key requirement, as they have a strong impact on the performance and the lifetime of the control system. By using the double integrator model (10), under the assumption that the disturbance τ_d is approximately constant with respect to the error dynamics time constants, it is shown in [12], [13]

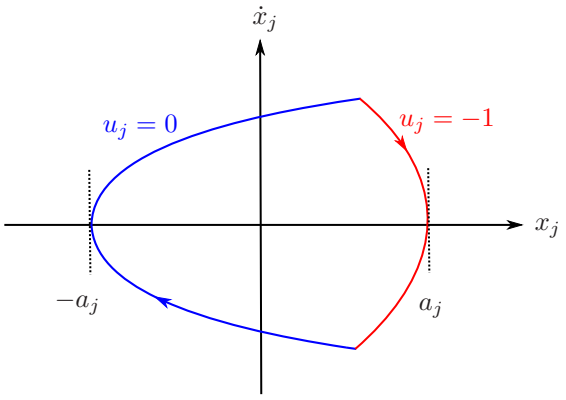

Fig. 1. Limit cycle corresponding to (15).

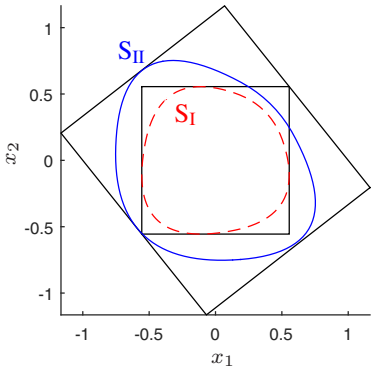

Fig. 2. Trajectories in the x_1, x_2 plane corresponding to the solutions S_I (dashed) and S_{II} (solid), with constraints $\|Cx\|_\infty \leq 1$ (outer parallelotope).

that the determination of the fuel/switch-optimal trajectories, satisfying (12), requires the solution of the following mixed-integer optimization problem

$$\begin{aligned} \min_{u} \ \max_{j} \ \lim_{T\to\infty} \frac{1}{T}\int_0^T |\dot{u}_j(t)|\,dt \\ \text{s.t.} \quad \ddot{x}(t) = u(t) + d \\ \|C\,x(t)\|_\infty \leq 1 \\ u(t) \in \{-1, 0\}^3, \end{aligned} \tag{13}$$

where $x = G^{-1}B^{-1}I_M\,\delta\theta$, $u = G^{-1}\,\mu$, $d{=}G^{-1}\,\varrho$, $\varrho = B^{-1}\,\tau_d$, $C = WI_M^{-1}BG$ and $G = \text{diag}(\text{sgn}(\varrho))$. As a consequence, $d_j \geq 0$. Hereafter, we will assume $d_j > 0$, since in the trivial case $d_j = 0$ the system can be controlled to the origin in finite time using well-known results from the literature [15]. Notice that the integral in (13) corresponds to the number of switchings that the binary signal u_j makes over the considered time horizon. In problem (13), the dynamics are decoupled, but the state constraints are coupled if the input matrix B is not diagonal. This occurs frequently in applications, e.g., whenever non-orthogonal thruster configurations are adopted, in order to meet constraints coming from the spacecraft layout or to maximize the efficiency of the attitude control system. In such cases, problem (13) becomes very challenging despite the simple dynamics.

C. Reference trajectory

The solution to the single-axis version of problem (13) (i.e. $x \in \mathbb{R}$) is a periodic trajectory [15], [16]. By building on this, in [12] two suboptimal solutions to the multi-axis version of problem (13) have been proposed. For system

$$\ddot{x}_j(t) = u_j(t) + d_j, \quad j = 1, 2, 3, \tag{14}$$

the reference trajectory is parameterized as

$$\begin{aligned} x_j(t) &= a_j\, f_j(\lambda_j), \\ \lambda_j &= \text{mod}(t/p + \phi_j, 1), \\ a_j &= p^2\,\gamma_j, \\ \gamma_j &= d_j(1 - d_j)/16, \end{aligned} \tag{15}$$

where

$$f_j(\lambda_j) = \begin{cases} 1 - \frac{8}{d_j}\,(\lambda_j - \frac{d_j}{2})^2 & \text{if } 0 \leq \lambda_j \leq d_j \\ -1 - \frac{8}{d_j - 1}(\lambda_j - \frac{d_j+1}{2})^2 & \text{if } d_j < \lambda_j < 1. \end{cases}$$

In (15), the parameter p represents the period of the trajectory and is equal for all axes, while $\phi_j \in [0, 1)$ is the phase and a_j denotes the amplitude. This corresponds to the limit cycle depicted in Fig. 1. Notice that, in order to make x_j evolve along such a trajectory, two input switchings per period are necessary.

The first suboptimal solution of (13), denoted by S_I, optimizes the switching frequency $2/p$ over the period p. Such an approach is rather conservative, as it amounts to constrain the trajectory in an axis-aligned box $|x_j| \leq p^2\gamma_j$, inscribed in the parallelotopic set $\|C\,x(t)\|_\infty \leq 1$.

The second strategy takes advantage of the additional degree of freedom provided by the phases ϕ_j of the trajectories (15). The resulting solution, denoted by S_{II}, is guaranteed to have larger amplitudes a_j of the oscillations and therefore a smaller switching frequency. To illustrate this fact, the S_I and S_{II} solutions for a two-axis example are compared in Fig. 2. It can be clearly seen that the control requirement $\|Cx\|_\infty \leq 1$ is met in both cases. However, the state trajectory corresponding to S_I is constrained to lie inside a smaller region, which yields a higher switching frequency.

III. Minimum switching control law

In this section, the control law under evaluation is briefly recalled. The interested reader is referred to [13] for further details. First, let us show how to steer system (14) to the trajectory (15), by tracking only the period p (this corresponds to solution S_I). For ease of exposition, hereafter the subscript j is dropped from the notation (e.g., it is left intended that $x = x_j \in \mathbb{R}$). The following control law, termed MS_I, can be adopted from the literature [17]

$$\text{MS}_\text{I}: \quad u(t) = \begin{cases} -1 & \text{if} \quad s(x, \dot{x}) \geq a \\ 0 & \text{if} \quad s(x, \dot{x}) \leq -a \\ u_p & \text{otherwise,} \end{cases} \tag{16}$$

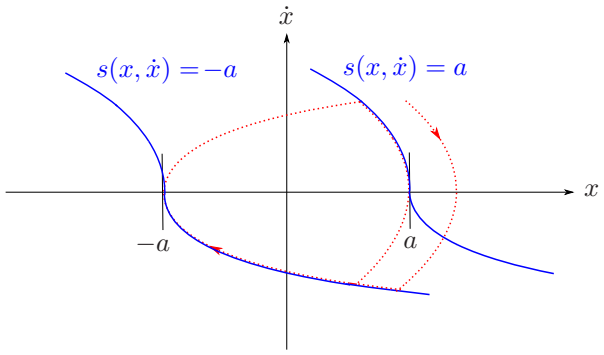

Fig. 3. Switching curves (solid) and example of a trajectory (dotted) from the application of the MS_I control law.

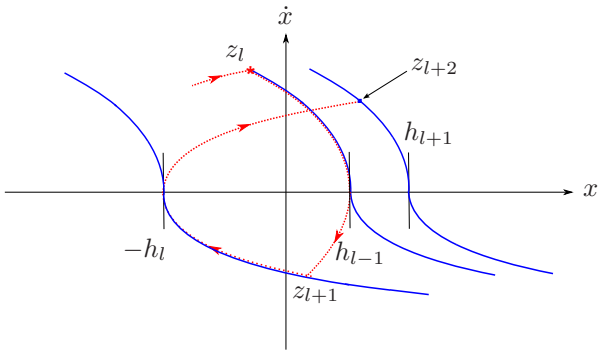

Fig. 4. Switching curves (solid) and example of a trajectory (dotted) from the application of the MS_{II} control law.

where $u_p = -1$ if $s(x,\dot{x}) \geq a$ occurred more recently than $s(x,\dot{x}) \leq -a$, $u_p = 0$ otherwise. Moreover, $a = p^2\gamma$ and

$$s(x,\dot{x}) = \begin{cases} x - \frac{1}{2(d-1)}\dot{x}^2 & \text{if} \quad \dot{x} \geq 0 \\ x - \frac{1}{2d}\dot{x}^2 & \text{if} \quad \dot{x} < 0 \end{cases} \tag{17}$$

is the classical fuel-optimal switching function (see e.g. [18]). The resulting closed-loop system consists of the system (14), under the relay feedback (16)-(17), with fixed hysteresis parameter a.

The switching curves $s(x,\dot{x}) = a$ and $s(x,\dot{x}) = -a$ are reported in the phase plane in Fig. 3, together with a trajectory example (dotted). By analysing the phase portrait in Fig. 3, it is evident that, by applying the control law MS_I to each axis of the perturbed double integrator (14), the closed-loop trajectory converges in finite time to the class of periodic trajectories provided by S_I. Moreover, only one switching per input channel is required to reach these trajectories from any initial condition.

In order to achieve the less conservative solution S_{II}, also a prescribed phase ϕ must be tracked. This can be done by using a time-varying hysteresis defined by parameters $a^U(t)$ and $a^L(t)$. To this purpose, the control law (16) is modified as

$$\text{MS}_{\text{II}}: \quad u(t) = \begin{cases} -1 & \text{if} \quad s(x,\dot{x}) \geq a^U(t) \\ 0 & \text{if} \quad s(x,\dot{x}) \leq -a^L(t) \\ u_p & \text{otherwise,} \end{cases} \tag{18}$$

where $u_p = -1$ if $s(x,\dot{x}) \geq a^U(t)$ occurred more recently than $s(x,\dot{x}) \leq -a^L(t)$, and $u_p = 0$ otherwise, with $a^L(t) + a^U(t) > 0$. The idea is to update the parameter defining the offset of a switching curve whenever the opposite curve is reached, so as to obtain a cycle with the desired phase and period. This results in piece-wise constant parameters $a^L(t)$ and $a^U(t)$

$$\begin{array}{ll} a^L(t) = h_{2m-1} & \text{for } t \in [z_{2m-1},\, z_{2m+1}), \\ a^U(t) = h_{2m} & \text{for } t \in [z_{2m},\, z_{2m+2}). \end{array} \tag{19}$$

where the sequence $\{z_l\}$ denotes the time instants at which the state trajectory reaches a switching curve (see Fig. 4). The design of the the sequence $\{h_l\}$ defining the parameters $a^L(t)$ and $a^U(t)$ is given by the following recursion

$$h_0 = a, \tag{20}$$

$$h_l = a\left(1 + 4\Delta\phi_l + 2\Delta\phi_l^2\right), \tag{21}$$

where

$$\Delta\phi_l = \text{mod}\left(\frac{\bar{z}_{l+2} - \hat{z}_{l+2}}{p} + \frac{1}{2},\, 1\right) - \frac{1}{2}, \tag{22}$$

$$\hat{z}_{l+2} = z_l + \frac{|\dot{x}(z_l)|}{q(z_l)} + \frac{q(z_l)}{2}p + \frac{\sqrt{2}}{4}\sqrt{p^2 + \frac{h_{l-1}}{\gamma}}, \tag{23}$$

$q(z_l) = |u(z_l) + d|$, and $\{\bar{z}_l\}$ is defined according to

$$\begin{array}{rcl} \bar{z}_{2m-1} & = & -\phi\, p, \\ \bar{z}_{2m} & = & (d-\phi)\, p. \end{array} \tag{24}$$

In [13], it has been shown that the single-axis solution of system (14) with the control law (18) converges in finite time to the periodic trajectory (15) with period p and phase ϕ. Moreover, only three switchings of the control input are required to reach this trajectory from any initial condition.

IV. LEO MISSION SIMULATIONS

In order to assess the feasibility of the proposed approach, a LEO space mission is simulated. The objective is to track an Earth-pointing attitude q_{IR} which is slowly rotating at an angular rate $\omega_R = [0, 1, 0]^T$ mrad/s, corresponding to the orbit rate of the spacecraft, using a set of on-off thrusters delivering 1.5 mN of thrust each. The thruster configuration is similar to that employed in [5], resulting in

$$B = \begin{bmatrix} -0.7 & 0.7 & 0 \\ 0.7 & 0.7 & 0 \\ 0 & 0 & 1.4 \end{bmatrix} \cdot 10^{-3}$$

in (11). The required control accuracy of 0.5 mrad per axis is taken into account by setting $W = (0.5 \cdot 10^{-3})^{-1} I$ in (12), where I denotes the identity matrix.

The truth model for the simulation is given by (1)-(3), and the simulation step size is taken as $\Delta t_s = 0.1$ s. It is assumed that an estimate of the spacecraft attitude, angular rate and of the disturbance torque τ_d is available onboard the spacecraft, which is used in the computation of the control law. Attitude and angular rate estimation errors are taken into account by adding white noises to signal (4) and its derivative, with standard deviations given by $\sigma_\theta = 10$ μrad and $\sigma_{\dot{\theta}} = 0.1$

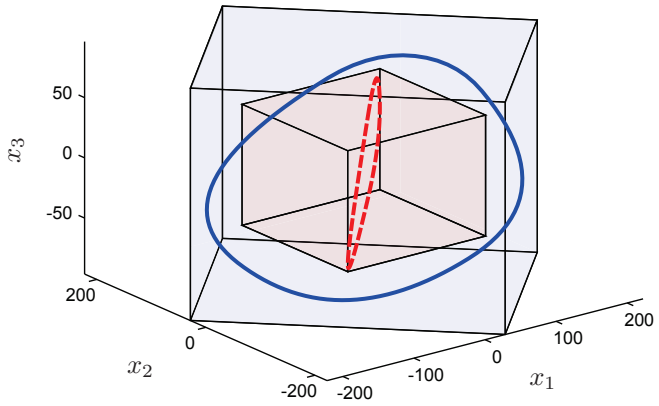

Fig. 5. Periodic trajectories corresponding to solutions S_I (red, dashed) and S_{II} (blue, solid), with state constraints $|x_j| \leq p^2\gamma_j$ (inner box) and $\|C\,x(t)\|_\infty \leq 1$ (outer parallelotope).

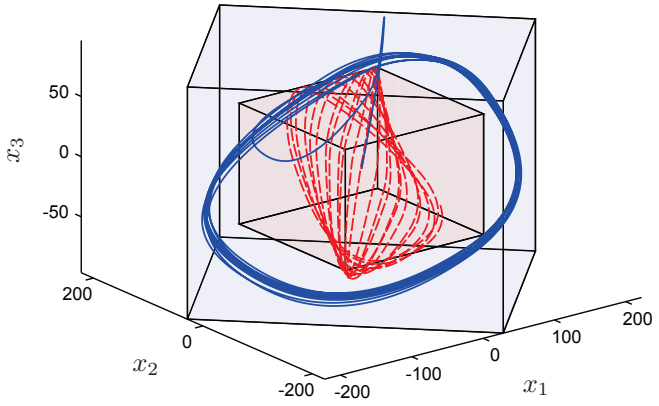

Fig. 6. Trajectories resulting from the application of the control schemes MS_I (red, dashed) and MS_{II} (blue, solid), with state constraints $|x_j| \leq p^2\gamma_j$ (inner box) and $\|C\,x(t)\|_\infty \leq 1$ (outer parallelotope).

μrad/s. Similarly, the disturbance torque estimation error is modeled as a white noise process with standard deviation $\sigma_\tau = 1\mu$N·m.

In the following, the performance of the control laws MS_I and MS_{II} are compared on two scenarios, featuring a constant or a slowly time-varying disturbance torque, respectively.

A. Constant disturbance

Let a constant disturbance torque $\tau_d = [0,\, 0.5,\, 0.2]^T$ mN·m, due to atmospheric drag, be the main perturbation acting on the spacecraft. The periodic trajectory provided by S_{II} (blue, solid) is depicted in terms of the variables x_1, x_2, x_3 in Fig. 5, together with the trajectory resulting from the more conservative solution S_I (red, dashed) and the outer parallelotope $\|C\,x(t)\|_\infty \leq 1$, representing the pointing accuracy requirements. The closed-loop trajectories, from the application of the control laws MS_I and MS_{II} are shown in Fig. 6, for a simulation of 2000 s. It can be seen that the trajectory given by MS_I (red, dashed) is maintained within the box specified by S_I, with few constraint violations caused by noise and discretization errors. Observe that, due to the presence of such contributions, the MS_I trajectory tends to move freely within the box, as the relative phases of the single-axis oscillations are not controlled. Conversely, the trajectory resulting from the application of the control scheme MS_{II} (blue, solid) closely follows the path prescribed by S_{II} after an initial transient, because in this case the relative phases are controlled.

The tracking error profiles are reported in Fig. 7, in terms of the roll, pitch and yaw error variables $\delta\theta_1$, $\delta\theta_2$ and $\delta\theta_3$. It can be seen that the pointing accuracy requirements are satisfied by both solutions. This confirms that the double integrator model (10) provides a good approximation of the attitude error dynamics, for the purpose of control design. The fuel consumption and switching frequency of the control systems are reported in Table I. The proposed control scheme performs better than the classical one, as expected. In particular, it provides a 18% reduction of the actuator switching frequency, while the fuel consumption is the same for both solutions (by construction).

TABLE I

CONTROL SYSTEM PERFORMANCE: CONSTANT DISTURBANCE

Control law	Firing time (fuel consumption)	Switching freq.
MS_I	1800 s (sum of all actuators)	24.0 mHz
MS_{II}	1800 s (sum of all actuators)	19.7 mHz

B. Time-varying disturbance

The case in which an additional time-varying disturbance acts on the system, due to a large residual magnetic dipole of the spacecraft, is addressed within the LEO mission scenario considered in the previous case study. A sinusoidal disturbance τ_d, with an amplitude of 0.1 mN·m per axis, is assumed. The period of the disturbance is equal to about 90 minutes, which corresponds to the orbital period. Because of the slow variation of the disturbance, with respect to the attitude error dynamics timescale, the control schemes presented in this paper can still be applied, provided that S_I and S_{II} are evaluated sufficiently often (e.g., twice per cycle, in correspondence of the switching events). Note that the numerical evaluation of S_{II} can take as low as 10 ms on a 2 Ghz, single core CPU. Consequently, both the reference period and phase, to be tracked by the control law MS_{II}, become time-varying.

The system is simulated for 6000 s. The attitude error profiles resulting from the application of MS_I and MS_{II} is reported in Fig. 8. It can be seen that the two approaches are able to keep the attitude error within the pointing accuracy bounds, for the entire simulation length. This suggests an appreciable robustness of the proposed approach to unmodeled dynamics and time-varying disturbances.

The fuel consumption and switching frequency, obtained with the two control schemes, are reported in Table II. Once again, the fuel consumption is the same for both solutions, while the control law MS_{II} performs better than MS_I in terms of switching cycles. In particular, a 20% reduction of on/off switching frequency is achieved, which translates into an

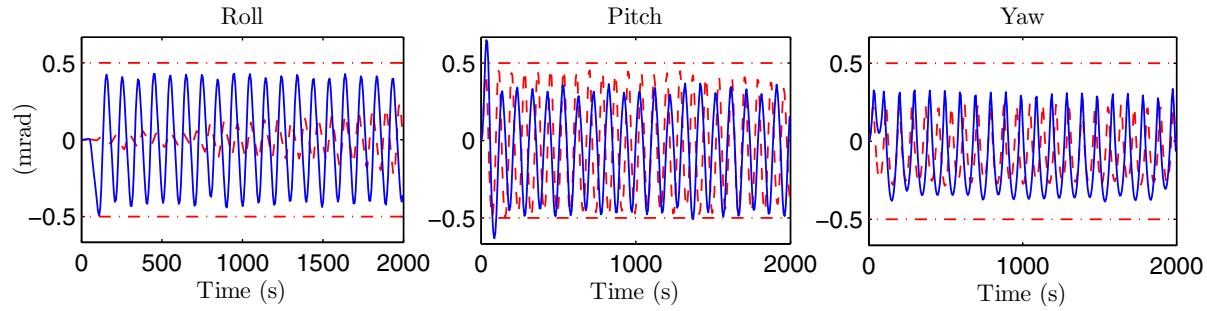

Fig. 7. Tracking error profile with constant disturbance: MS_I (red, dashed) and MS_{II} (blue, solid) control schemes.

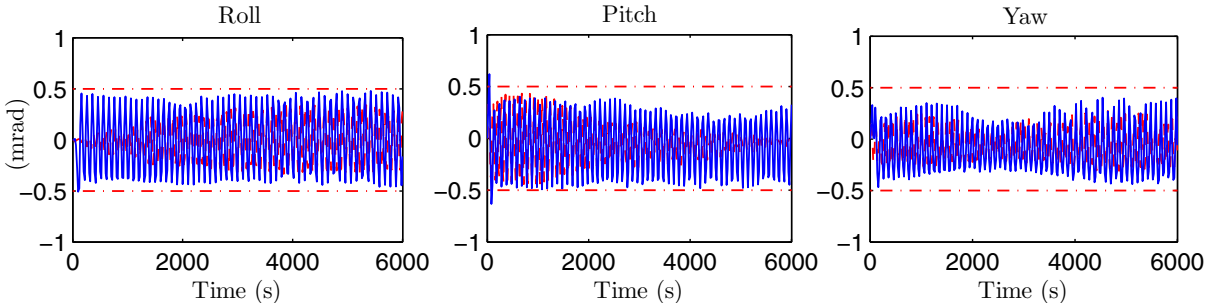

Fig. 8. Tracking error profile with time-varying disturbance: MS_I (red, dashed) and MS_{II} (blue, solid) control schemes.

TABLE II
CONTROL SYSTEM PERFORMANCE: TIME-VARYING DISTURBANCE

Control law	Firing time (fuel consumption)	Switching freq.
MS_I	5400 s (sum of all actuators)	24.4 mHz
MS_{II}	5400 s (sum of all actuators)	19.5 mHz

increased performance and lifetime of the thrusters.

V. CONCLUSIONS

This paper has presented the evaluation of a minimum fuel and minimum switching control law for three-axis precision pointing of spacecraft with on/off actuators. The results from a simulation case study of a low Earth orbit mission demonstrate the feasibility of the proposed approach when applied to the problem of tracking a rotating reference within a given accuracy, while rejecting constant or slowly time-varying disturbances. The obtained results are encouraging, in view of the limited computational effort. Future work will aim at investigating the robustness of the control law, as well as the extension of the proposed approach to attitude reorientation problems.

REFERENCES

[1] M. Coletti, A. Grubisic, C. Collingwood, N. Wallace, N. Wells, and S. Gabriel, "European student moon orbiter solar electric propulsion subsystem architecture: An all-electric spacecraft," *Acta Astronautica*, vol. 65, no. 3, pp. 354–364, 2009.

[2] S. A. Feuerborn, D. Neary, and J. Perkins, "Finding a way: Boeing's all electric propulsion satellite," in *49th AIAA/ASME/SAE/ASEE Joint Propulsion Conference & Exhibit*, San Jose, California, 2013.

[3] D. Nicolini, D. Robertson, E. Chesta, G. Saccoccia, D. Gibbon, and A. M. Baker, "Xenon resistojets as a secondary propulsion on EP spacecrafts and performance results of resistojets using xenon," in *28th International Electric Propulsion Conference*, Toulouse, France, 2003.

[4] T. Krøvel, F. Dörfler, M. Berger, and J. Rieber, "High-precision spacecraft attitude and manoeuvre control using electric propulsion," in *60th International Austronautical Congress*, Daejeon, Republic of Korea, 2009.

[5] M. Leomanni, A. Garulli, A. Giannitrapani, and F. Scortecci, "All-electric spacecraft precision pointing using model predictive control," *Journal of Guidance, Control, and Dynamics*, vol. 38, no. 1, pp. 161–168, 2015.

[6] P. Gessini, M. Coletti, A. Grubisic, S. Gabriel, N. Wallace, and D. Fearn, "Hollow cathode thruster for all-electric spacecraft," in *43rd AIAA/ASME/SAE/ASEE Joint Propulsion Conference & Exhibit*, Cincinnati, Ohio, 2007.

[7] W. Wright and P. Ferrer, "Electric micropropulsion systems," *Progress in Aerospace Sciences*, vol. 74, pp. 48 – 61, 2015.

[8] X. Xu and P. J. Antsaklis, "Optimal control of switched systems based on parameterization of the switching instants," *IEEE Transactions on Automatic Control*, vol. 49, no. 1, pp. 2–16, 2004.

[9] M. Egerstedt, Y. Wardi, and H. Axelsson, "Transition-time optimization for switched-mode dynamical systems," *IEEE Transactions on Automatic Control*, vol. 51, no. 1, pp. 110–115, 2006.

[10] X. Ding, Y. Wardi, D. Taylor, and M. Egerstedt, "Optimization of switched-mode systems with switching costs," in *Proceedings of the American Control Conference*, Seattle, Washington, 2008, pp. 3965–3970.

[11] B. Solberg, P. Andersen, J. M. Maciejowski, and J. Stoustrup, "Optimal switching control of burner setting for a compact marine boiler design," *Control Engineering Practice*, vol. 18, no. 6, pp. 665–675, 2010.

[12] A. Garulli, A. Giannitrapani, and M. Leomanni, "Minimum switching limit cycle oscillations for systems of coupled double integrators," in *Proceedings of the 53rd IEEE Conference on Decision and Control*, Los Angeles, California, 2014, pp. 4655 – 4660.

[13] ——, "Minimum switching control for systems of coupled double integrators," *Automatica*, vol. 60, pp. 115 – 121, 2015.

[14] M. E. Pittelkau, "Rotation vector in attitude estimation," *Journal of Guidance, Control, and Dynamics*, vol. 26, no. 6, pp. 855–860, 2003.

[15] M. Athans, "Minimum-fuel feedback control systems: second-order case," *IEEE Transactions on Applications and Industry*, vol. 82, no. 65, pp. 8–17, 1963.

[16] M. H. Kaplan, *Modern Spacecraft Dynamics and Control*. John Wiley and Sons, 1976.

[17] S. Dodds, "Adaptive, high precision, satellite attitude control for microprocessor implementation," *Automatica*, vol. 17, no. 4, pp. 563–573, 1981.

[18] M. Athans and P. L. Falb, *Optimal Control: An Introduction to the Theory and its Applications*. Courier Dover Publications, 2006.